

## ***Achyranthes aspera*-Mediated Silver Nanoparticle Synthesis for Enhanced Enrichment: Toxicological Studies on *Eudrilus eugeniae* Earthworms**

**Thayalan Uma RAJALAKSHMI<sup>1</sup>, Chellaiah ESAIVANI<sup>2</sup>, Thangaiya ANANTHAKUMAR<sup>3</sup>, Sami Al OBAID<sup>4</sup>, Hossam M. ALJAWDAH<sup>5</sup>, Ramaiah MARISELVAM<sup>6</sup>\***

<sup>1</sup> PG and Research Department of Chemistry, Rani Anna Government College for Women, Tirunelveli – 627008, Tamil Nadu, India

<sup>2</sup> PG Department of Zoology, Sarah Tucker College (Autonomous), Tirunelveli. Affiliated to M.S. University, Tirunelveli, Tamil Nadu, India

<sup>3</sup> Department of Chemistry, Merit Arts and Science College, Idaikkal, Tirunelveli, Tamil Nadu, India – 627602

<sup>4</sup> Department of Botany and Microbiology, College of Science, King Saud University, PO Box -2455, Riyadh -11451, Saudi Arabia

<sup>5</sup> Department of Zoology, College of Science, King Saud University, P.O. Box 2455, Riyadh 11451, Saudi Arabia

<sup>6</sup> Saraswathi Institute of Lifescience, Terkkumadathur, Tenkasi – 627423, Tamil Nadu, India

<http://doi.org/10.5755/j02.ms.36170>

Received 26 January 2024; accepted 7 March 2024

This study utilizes gas chromatography mass spectrometry (GC-MS) to analyze phytochemicals in *Achyranthes aspera*, revealing over 57 phyto components in its methanol extracts. Major components include Neophytadiene, Stigmasterol, and Lupeol. The study then explores the formation of silver nanoparticles (AgNPs) using these extracts, observing a color change in the reaction mixture, indicating successful synthesis. UV/Vis spectra reveal absorption peaks at 343 and 411 nm, indicative of surface plasmon resonance (SPR) in the AgNPs. Fourier-transform infrared spectroscopy (FTIR) highlights various functional groups present in the nanoparticles. X-ray diffraction (XRD) confirms the crystalline nature of the AgNPs, showing distinct peaks corresponding to crystallographic planes. SEM and AFM images display spherical AgNPs with cluster formations. The introduction of these plant-mediated AgNPs to earthworms results in significant growth compared to control groups. Silver content analysis in earthworms corroborates the effectiveness of the plant-mediated nanoparticles. Dissection analysis reveals enhanced growth in reproductive organs. Despite the benefits of nanomaterials, the study acknowledges potential toxicological concerns, emphasizing the increasing usage of silver nanoparticles and their potential impact on the environment. This research provides valuable insights into the synthesis, characterization, and biological effects of plant-mediated silver nanoparticles.

**Keywords:** silver nanoparticles, *Eudriluseugeniae*, toxicology, reproductive organ.

### **1. INTRODUCTION**

Nanotechnology is the science and engineering of manipulating matter at the nanoscale, which is typically between 1 and 100 nanometers (nm) in size [1]. It involves the design, production, and application of structures, devices, and systems by controlling the properties of materials at the atomic and molecular level [2]. The unique properties of materials at the nanoscale have led to the development of many applications in various fields, including medicine, electronics, energy, and the environment [3–5].

One of the most significant areas of nanotechnology research is the synthesis and application of nanoparticles. Nanoparticles are particles with at least one dimension less than 100 nm, and they can be synthesized using various methods, such as chemical, physical, or biological [6]. Nanoparticles have unique properties due to their small size, such as high surface area to volume ratio, quantum confinement, and surface effects, which make them suitable for various applications, such as drug delivery, imaging, and sensors [7].

However, the increasing production and use of nanoparticles have raised concerns about their potential toxicity to human health and the environment [8]. Nanoparticle toxicity is a complex issue that involves the physicochemical properties of nanoparticles, exposure routes, and biological responses [9]. The toxicity of nanoparticles can occur through various mechanisms, such as oxidative stress, inflammation, genotoxicity, and cell death, which can lead to adverse effects on human health and the environment [10].

#### **1.1. Properties and synthesis methods of nanoparticles**

Nanoparticles can be synthesized using various methods, such as chemical, physical, or biological. Chemical methods involve the reduction of metal salts in the presence of stabilizing agents, such as surfactants, to control the size and shape of nanoparticles [11]. Physical methods involve the evaporation or condensation of metals in a vacuum or inert gas environment, such as laser ablation or sputtering [12]. Biological methods involve the use of living

\*Corresponding author. Tel.: +91-8012261469.

E-mail: [r.mariselvam@silsorg.in](mailto:r.mariselvam@silsorg.in)(R. Mariselvam)

organisms, such as bacteria or plants, to synthesize nanoparticles through the reduction of metal ions [13].

## 1.2. Potential applications of nanoparticles

Nanoparticles have many potential applications in various fields, such as medicine, electronics, energy, and the environment [14]. In medicine, nanoparticles can be used for drug delivery, imaging, and therapy. For example, liposomal nanoparticles can encapsulate drugs and deliver them to specific sites in the body, while magnetic nanoparticles can be used for magnetic resonance imaging and hyperthermia therapy [15]. In electronics, nanoparticles can be used for the fabrication of elements of nanoelectronics, such as transistors and memory devices [16]. In energy, nanoparticles can be used for the production and storage of energy, such as solar cells and batteries [17]. In the environment, nanoparticles can be used for water treatment, pollution remediation, and sensing [18].

## 1.3. Mechanisms of nanoparticle toxicity

Nanoparticles have unique properties such as high surface area, reactivity, and ability to cross biological barriers that make them useful in various fields. However, their small size also makes them more toxic than larger particles. Understanding the mechanisms of nanoparticle toxicity is crucial for the safe development and application of nanotechnology [19].

One of the primary mechanisms of nanoparticle toxicity is oxidative stress. Nanoparticles can induce the production of reactive oxygen species (ROS) such as hydrogen peroxide and superoxide, which can damage cellular components such as DNA, proteins, and lipids. This can lead to inflammation, cell death, and the development of diseases such as cancer, neurodegenerative disorders, and cardiovascular disease [20].

Another mechanism of nanoparticle toxicity is genotoxicity. Nanoparticles can interact with DNA and cause mutations or chromosomal damage. This can lead to the development of cancer and other genetic diseases [21].

Nanoparticles can also disrupt cellular signaling pathways. They can interact with cell membrane receptors and interfere with normal cellular signaling, leading to cell death or abnormal cellular function. Additionally, nanoparticles can interfere with intracellular signaling pathways, leading to the dysregulation of important cellular processes such as cell growth and differentiation [22].

Nanoparticles can also cause inflammation. They can activate immune cells and stimulate the release of inflammatory cytokines, leading to chronic inflammation. Chronic inflammation is associated with the development of various diseases such as asthma, cardiovascular disease, and cancer [23].

Nanoparticles can also cause toxicity through their physical properties. For example, nanoparticles can penetrate through biological barriers and accumulate in organs such as the liver, spleen, and lungs. This can cause organ damage and dysfunction. Additionally, nanoparticles can cause mechanical damage to cells and tissues due to their small size and high surface area [24].

This study was focused on the toxicity of the plant mediated silver nanoparticles on Indian earthworm *E.eugenia*.

## 2. MATERIALS AND METHODS

### 2.1. Preparation of plant mediated silver nanoparticles

Ninety milliliters of 0.1 mM silver nitrate solution were prepared using double distilled water. The plant sample, *Achyranthes aspera* (L) was collected from Coutrallam region (GPS Coordinates: 8°55'35.652" N and 77°16'2.028" E), Tenkasi, Tamil Nadu, India. The collected material was shade dried and extracted using methanol as a solvent. The excess amount of methanol was removed using a Soxhlet apparatus to form the crude extract. The plant extract was analyzed their phytochemicals through GC-MS (SHIMADZU). The crude extract dissolved in double distilled water for nanoparticle synthesis. Add ten milliliters of plant sample mixed with the ninety milliliters of silver nitrate solution. The mixture was kept at room temperature for 24 hours. After 24 h the bio-reduced silver nitrate solution became brown indicating the synthesis of silver nanoparticles.

### 2.2. Characterization and size of plant mediated silver nanoparticles

The spectral and advanced microscope was used to analyze the physical and structural characterization of nanoparticles. The prepared *A. aspera* plant extract-based silver nanoparticles were characterized by UV/Vis spectrophotometer (Systronics-2203), FT-IR (JASCO), SEM (Zeiss EVO 18), AFM (Agilent 5100) and XRD (X'Pert Pro – PAnalytic).

### 2.3. Toxicological experimental setup

Experiment 1: the selected Indian earthworm species *Eudrilus eugeniae* was selected for this study. Earthworms are divided into two groups, each group containing 3 earthworms. Around 200 µl of plant mediated prepared silver nanoparticles are injected in one group for seven days and another one is in control. Every day the earthworm's growth rate was measured.

Experiment 2: the selected earthworm species divided into five groups and each group contains three earthworms. 200 µl of green synthesized silver nanoparticles were injected into each group. Silver levels in earthworms were calculated using UV/visible spectral study at 1 h, 2 h, 24 h, 168 h and 216 h.

Experiment 3: 200 µl of silver nanoparticles were injected into one group of earthworms and another one group was control. After seven days of injection the earthworms were dissected at clitellum range using a sterile blade and observed inner reproductive organs.

## 3. RESULTS AND DISCUSSION

The gas chromatography mass spectrum is a powerful analytical instrument, to analyze the phytochemicals present in the test plant samples. The methanol extracts of *A. aspera* had more than 57 different phyto components confirmed by GC-MS (Fig. 1 and Table 1). The major components are Neophytadiene, Stigmasterol, 9,19-Cycloergost-24(28)-en-3-ol, 4,14-dimethyl, 22,23-Dibromostigmasterol acetate, 9,19-Cyclolanostan-3-ol, acetate, (3.β.)-Lupeol, and Methyl oleate.

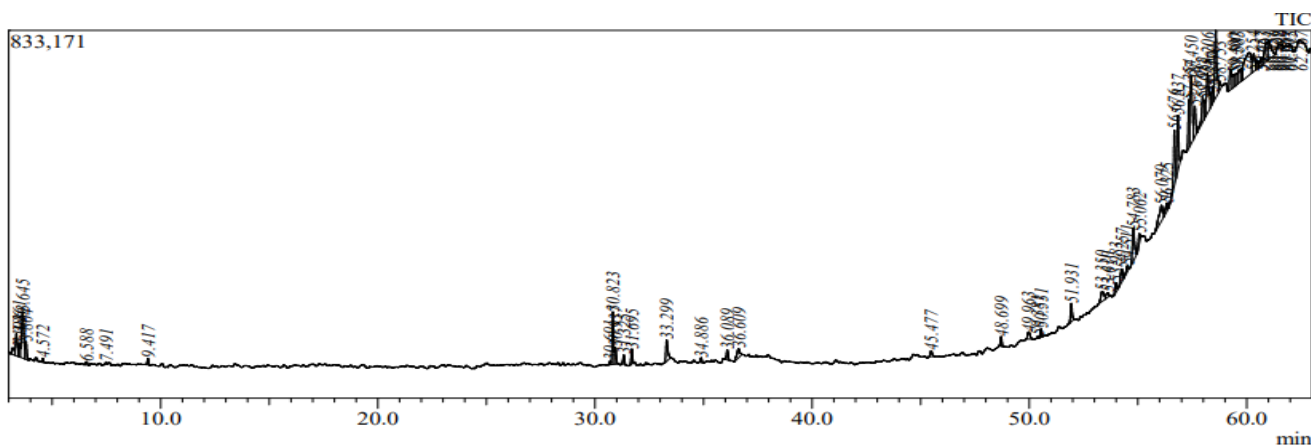


Fig. 1. GC-MS analysis of *A. aspera* plant extract

Table 1. Peak report of GC-MS analysis

| Peak# | R.Time | I.Time | F.Time | Area     | Area%  | Height  | Height% | A/H Name  |
|-------|--------|--------|--------|----------|--------|---------|---------|---|
| 1     | 3.191  | 3.103  | 3.287  | 110660   | 0.71   | 15154   | 0.65    | 7.30 Octane, 2,7-dimethyl-                        |
| 2     | 3.361  | 3.287  | 3.433  | 274721   | 1.77   | 50830   | 2.17    | 5.40 3,4-Dimethyl-2-hexene                        |
| 3     | 3.486  | 3.433  | 3.543  | 163624   | 1.05   | 29053   | 1.24    | 5.63 2,4-Dimethyl-1-hexene                        |
| 4     | 3.645  | 3.543  | 3.753  | 729726   | 4.69   | 104575  | 4.46    | 6.98 2-Hexene, 2,5-dimethyl-                      |
| 5     | 3.804  | 3.753  | 3.927  | 195143   | 1.25   | 40108   | 1.71    | 4.87 3-Hexene, 3,4-dimethyl-, (Z)-                |
| 6     | 4.572  | 4.503  | 4.667  | 39904    | 0.26   | 9307    | 0.40    | 4.29 Acetic acid, butyl ester                     |
| 7     | 6.588  | 6.517  | 6.700  | 40859    | 0.26   | 7861    | 0.34    | 5.20 Methyl cis-11-icosenoate                     |
| 8     | 7.491  | 7.430  | 7.560  | 20810    | 0.13   | 5201    | 0.22    | 4.00 Methyl cis-11-icosenoate                     |
| 9     | 9.417  | 9.343  | 9.510  | 61518    | 0.40   | 14453   | 0.62    | 4.26 Decane                                       |
| 10    | 30.691 | 30.620 | 30.737 | 32906    | 0.21   | 7676    | 0.33    | 4.29 1-Decene, 3,3,4-trimethyl-                   |
| 11    | 30.823 | 30.737 | 30.893 | 564808   | 3.63   | 118791  | 5.06    | 4.75 Neophytadiene                                |
| 12    | 30.937 | 30.893 | 31.053 | 189526   | 1.22   | 38188   | 1.63    | 4.96 3,7,11,15-Tetramethylhexadec-2-ene           |
| 13    | 31.325 | 31.240 | 31.437 | 97604    | 0.63   | 20984   | 0.89    | 4.65 3-Methylene-7,11-dimethyl-1-dodecene         |
| 14    | 31.695 | 31.603 | 31.780 | 154090   | 0.99   | 34236   | 1.46    | 4.50 3,7,11,15-Tetramethyl-2-hexadecen-1-ol       |
| 15    | 33.299 | 33.207 | 33.490 | 311090   | 2.00   | 48374   | 2.06    | 6.43 n-Hexadecanoic acid                          |
| 16    | 34.886 | 34.817 | 34.983 | 45677    | 0.29   | 10304   | 0.44    | 4.43 Palmitic acid-TMS                            |
| 17    | 36.089 | 36.010 | 36.230 | 115732   | 0.74   | 23167   | 0.99    | 5.00 Phytol                                       |
| 18    | 36.609 | 36.413 | 36.770 | 205402   | 1.32   | 20422   | 0.87    | 10.06 10-Methyldodec-2-en-4-olide                 |
| 19    | 45.477 | 45.393 | 45.637 | 77524    | 0.50   | 13098   | 0.56    | 5.92 Oxirane, heptadecyl-                         |
| 20    | 48.699 | 48.610 | 48.790 | 102400   | 0.66   | 22245   | 0.95    | 4.60 Eicosane                                     |
| 21    | 49.963 | 49.867 | 50.160 | 126489   | 0.81   | 16140   | 0.69    | 7.84 Methyl cis-11-icosenoate                     |
| 22    | 50.381 | 50.327 | 50.440 | 15414    | 0.10   | 4227    | 0.18    | 3.65 Methyl erucate                               |
| 23    | 50.531 | 50.443 | 50.613 | 85782    | 0.55   | 19046   | 0.81    | 4.50 Squalene                                     |
| 24    | 51.931 | 51.827 | 52.057 | 217753   | 1.40   | 41667   | 1.78    | 5.23 2-Methylhexacosane                           |
| 25    | 53.350 | 53.177 | 53.487 | 229112   | 1.47   | 22799   | 0.97    | 10.05 Methyl eicosa-8,11,14-trienoate             |
| 26    | 53.610 | 53.487 | 53.703 | 97284    | 0.63   | 10021   | 0.43    | 9.71 Methyl gamma-linolenate                      |
| 27    | 53.983 | 53.900 | 54.060 | 104749   | 0.67   | 21471   | 0.92    | 4.88 Phenol-TMS                                   |
| 28    | 54.257 | 54.060 | 54.340 | 199009   | 1.28   | 28415   | 1.21    | 7.00 6,6-Diethylheptadecane                       |
| 29    | 54.511 | 54.340 | 54.580 | 81949    | 0.53   | 13290   | 0.57    | 6.17 Methyl cis-11,14-Icosadienoate               |
| 30    | 54.783 | 54.647 | 54.943 | 522483   | 3.36   | 74712   | 3.19    | 6.99 2-Methylhexacosane                           |
| 31    | 55.062 | 54.970 | 55.127 | 114155   | 0.73   | 22951   | 0.98    | 4.97 4-Cresol-TMS                                 |
| 32    | 56.079 | 55.760 | 56.180 | 429527   | 2.76   | 35420   | 1.51    | 12.13 Methyl cis-11-icosenoate                    |
| 33    | 56.325 | 56.180 | 56.403 | 148060   | 0.95   | 18660   | 0.80    | 7.93 Docosapentaenoic acid-TMS                    |
| 34    | 56.676 | 56.490 | 56.753 | 664645   | 4.27   | 123834  | 5.28    | 5.37 Stigmasterol                                 |
| 35    | 56.837 | 56.753 | 56.947 | 673902   | 4.33   | 125173  | 5.34    | 5.38 9,19-Cycloergost-24(28)-en-3-ol, 4,14-dimeth |
| 36    | 57.354 | 57.237 | 57.377 | 477729   | 3.07   | 108373  | 4.62    | 4.41 Heptadecane                                  |
| 37    | 57.450 | 57.377 | 57.547 | 1065212  | 6.85   | 152583  | 6.51    | 6.98 22,23-Dibromostigmasterol acetate            |
| 38    | 57.618 | 57.547 | 57.720 | 402425   | 2.59   | 69301   | 2.95    | 5.81 Methyl eicosa-8,11,14-trienoate              |
| 39    | 57.982 | 57.730 | 58.033 | 382176   | 2.46   | 55854   | 2.38    | 6.84 Arachidonic acid-TMS                         |
| 40    | 58.073 | 58.033 | 58.117 | 187435   | 1.21   | 39742   | 1.69    | 4.72 Docosapentaenoic acid-TMS                    |
| 41    | 58.206 | 58.117 | 58.323 | 679677   | 4.37   | 90182   | 3.84    | 7.54 9,19-Cyclostan-3-ol, acetate, (3.beta.)-     |
| 42    | 58.370 | 58.323 | 58.410 | 157725   | 1.01   | 31357   | 1.34    | 5.03 Methyl cis-10-pentadecenoate                 |
| 43    | 58.470 | 58.410 | 58.497 | 174758   | 1.12   | 36470   | 1.55    | 4.79 Methyl cis-11-icosenoate                     |
| 44    | 58.583 | 58.497 | 58.707 | 984601   | 6.33   | 152012  | 6.48    | 6.48 Lupeol                                       |
| 45    | 58.753 | 58.707 | 58.863 | 130313   | 0.84   | 21077   | 0.90    | 6.18 Methyl linolelaidate                         |
| 46    | 59.254 | 59.153 | 59.343 | 332205   | 2.14   | 46599   | 1.99    | 7.13 Docosapentaenoic acid-TMS                    |
| 47    | 59.400 | 59.343 | 59.480 | 223559   | 1.44   | 29019   | 1.24    | 7.70 Methyl eicosa-8,11,14-trienoate              |
| 48    | 59.507 | 59.480 | 59.587 | 162148   | 1.04   | 27220   | 1.16    | 5.96 Methyl cis-10-heptadecenoate                 |
| 49    | 59.657 | 59.587 | 59.730 | 233826   | 1.50   | 29245   | 1.25    | 8.00 Methyl gamma-linolenate                      |
| 50    | 59.763 | 59.730 | 59.810 | 134347   | 0.86   | 28698   | 1.22    | 4.68 3-Aminopropanoic acid-2TMS                   |
| 51    | 60.131 | 59.810 | 60.243 | 1119749  | 7.20   | 50508   | 2.15    | 22.17 Methyl oleate                               |
| 52    | 60.329 | 60.243 | 60.427 | 324547   | 2.09   | 40100   | 1.71    | 8.09 Linoleic acid-TMS                            |
| 53    | 60.492 | 60.427 | 60.570 | 116851   | 0.75   | 18243   | 0.78    | 6.41 Methyl cis-11,14,17-Icosatrienoate           |
| 54    | 60.689 | 60.570 | 60.740 | 124479   | 0.80   | 16694   | 0.71    | 7.46 Methyl cis-13,16-Docosadienate               |
| 55    | 60.907 | 60.740 | 60.977 | 447825   | 2.88   | 43833   | 1.87    | 10.22 Methyl myristoleate                         |
| 56    | 61.015 | 60.977 | 61.310 | 436023   | 2.80   | 43031   | 1.83    | 10.13 Elaidic acid-TMS                            |
| 57    | 62.267 | 62.210 | 62.310 | 11690    | 0.08   | 3486    | 0.15    | 3.35 Methyl linolelaidate                         |
|       |        |        |        | 15553337 | 100.00 | 2345480 | 100.00  |   |

The formation of AgNPs by the reduction of  $\text{AgNO}_3$  during treatment with the plant extract is evident from the change in colour of the reaction mixture from colourless to brown colour which indicated the formation of AgNPs. The presence of different phytochemicals in the methanol extract of *A. aspera* influenced the reduction of  $\text{AgNO}_3$  to AgNPs. The presence of an absorption peak at 343 and 411 nm in the UV/Vis spectrum of silver nanoparticles points to the occurrence of surface plasmon resonance (SPR) (Fig. 2). This distinctive optical phenomenon arises from the coordinated movement of free electrons on the surface of the nanoparticles when they are reduced by plant extract. This synchronized electron oscillation is associated with the activation of surface plasmon resonances.

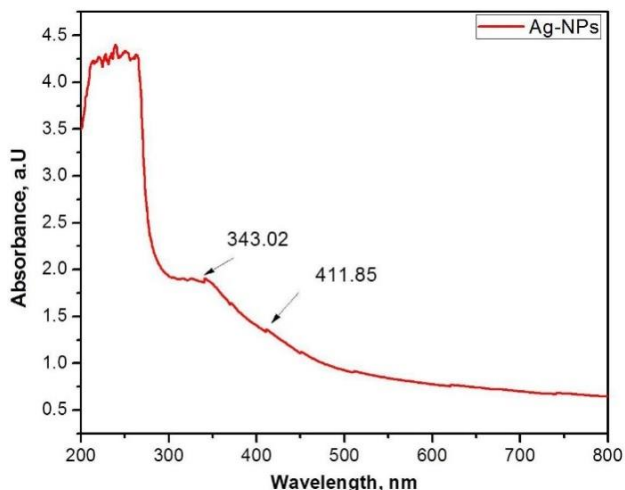


Fig. 2 UV/Vis spectra of green synthesized AgNPs

Silver nanoparticles, owing to their unique properties, particularly manifest this behavior in the UV region. The precise wavelength of the SPR peak is subject to variations influenced by factors such as the size, shape, and immediate environment of the nanoparticles. The fact that the absorption peak is situated at 343 and 411 nm implies that the silver nanoparticles possess a specific size or shape that leads to the manifestation of this resonance wavelength.

Analyzing the FTIR spectra of green-synthesized silver nanoparticles involves correlating the identified peaks with vibrational modes of functional groups that might exist on the nanoparticle surface or be associated with the stabilizing agents utilized in the synthesis process. The peaks recorded at 643.02, 914.87, 1005.49, 1327.80, 1368.78, 1498.91, 2980.13, and 3443.93  $\text{cm}^{-1}$  (Fig. 3) offer valuable insights. The peak at 643.02  $\text{cm}^{-1}$  may be linked to bending vibrations, potentially involving metal-oxygen bonds or interactions with stabilizing agents originating from the green synthesis. In the 914.87  $\text{cm}^{-1}$  region, there is a tendency for out-of-plane bending vibrations, suggesting a connection to stabilizing agents or organic molecules introduced during the green synthesis process. The peak at 1005.49  $\text{cm}^{-1}$  is typically associated with C-H bending vibrations, hinting at the presence of organic compounds from the green synthesis or surface-capping agents. The region around 1327.80  $\text{cm}^{-1}$  often corresponds to C-N stretching vibrations, implying the potential existence of amines or amides. At 1368.78  $\text{cm}^{-1}$ ,  $\text{CH}_3$  rocking vibrations are discernible, indicating the presence of methyl groups.

The peak at 1498.91  $\text{cm}^{-1}$  is frequently associated with C=C stretching vibrations in aromatic compounds. In the 2980.13  $\text{cm}^{-1}$  region, C-H stretching vibrations are typical, suggesting the presence of alkanes or alkyl groups. Finally, the peak at 3443.93  $\text{cm}^{-1}$  signifies O-H stretching vibrations, pointing to the presence of hydroxyl groups, which could be associated with stabilizing agents, biomolecules, or water molecules adsorbed on the nanoparticle surface.

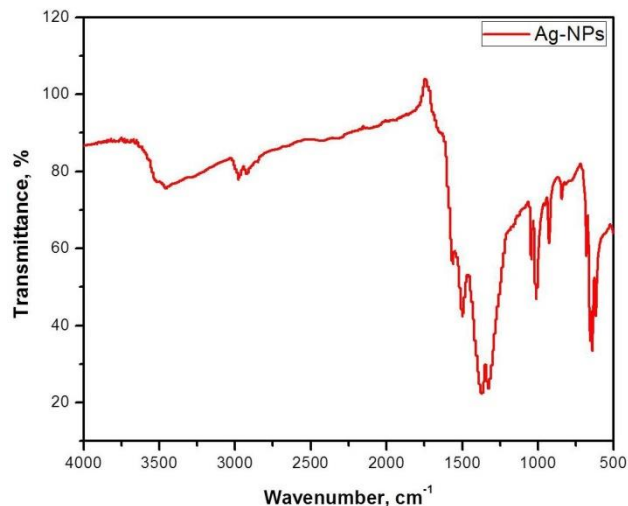


Fig. 3. FT-IR spectra of AgNPs

The XRD pattern of plant-based silver nanoparticles (Ag NPs) is illustrated in Fig. 4. The spectrum exhibits distinct and sharp peaks at 36.6, 43.9, 64.9, and 76.1° within the 10 to 80° range. These peaks correspond to the crystallographic planes (1 1 1), (2 0 0), (2 2 0), and (3 1 1), respectively. The presence of these well-defined peaks indicates the crystalline nature of the synthesized silver nanoparticles, suggesting a structured and organized arrangement of atoms within the nanoparticles. Additionally, our spectral data revealed the existence of a secondary phase, such as  $\text{Ag}_3\text{O}_4$ , among the silver nanoparticles. The crystalline planes associated with this secondary phase were also identified in Fig. 4.

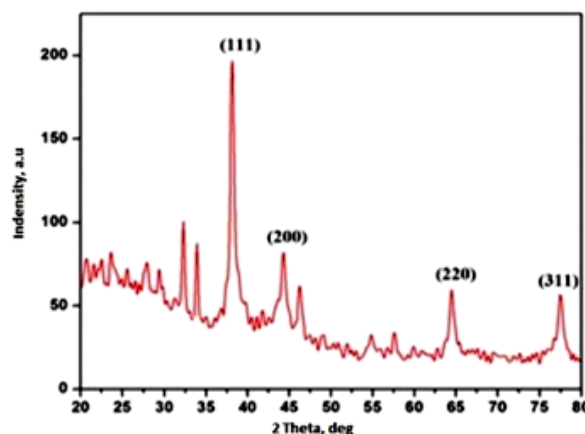
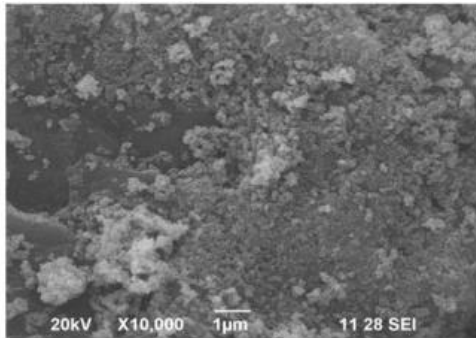


Fig. 4. XRD pattern of AgNPs

The surface morphology of green synthesized AgNPs was characterized by SEM and AFM images (Fig. 5 and Fig. 6). The synthesized nanoparticles are spherical in shape and cluster formation.

The plant mediated green synthesized silver nanoparticles injected earthworms have good growth compared to the control groups (Fig. 7 a and b). The initial weight of the earthworms group is 6.81 grams (each group contains 3 worms). In the treated group earthworm body weight is highly increased at 2<sup>nd</sup> day and 3<sup>rd</sup> day of treatment (Fig. 7 a). From the 3<sup>rd</sup> day to 6<sup>th</sup> day of the treated group earthworm growth rate slowly and slightly increased (Fig. 7 a). However, the control group earthworm growth rate is slightly increased (Fig. 7 b).



**Fig. 5.** SEM image of green synthesized AgNPs

Experiment 2 indicates the silver content level in earthworm body systems treated at plant mediated silver nanoparticles. The earthworm systems contain silver nanoparticles that are utilized by their system and quickly increase the growth (Fig. 7 a). The UV/Vis spectra study confirmed the silver level in treating group earthworms. Fig. 7 c indicates the silver level in the earthworm body system. On the first day treated earthworms body fluids OD value at 428 nm is more than one. After the 9<sup>th</sup> day of treated earthworms, the silver level was measured by UV/spectral studies. The OD value at 428 nm the 9<sup>th</sup> day of earthworms is decreased to less than 0.5. In this study the OD value was calculated at 428 nm. Because the prepared plant mediated silver nanoparticles are responsible at 428 nm in range

(Fig. 7 c).

The inner reproductive organ of silver nanoparticles treated and control earthworm (male and female reproductive part) was analyzed by dissection method. Fig. 8 a is plant mediated silver nanoparticles treated earthworm photo image. Label 1 is the seminal vesicle and Label 2 is the ovary and oviduct of the dissected earthworm. The seminal vesicle is a place for storing mature sperm. The seminal vesicle and ovary have better growth in comparison to the control earthworm (Fig. 8 b).

Expanding investigation of nanotechnology has resulted in the discovery of several unique properties of nanomaterials such as better magnetic [25], catalytic [26], optical [27], electrical [28] and mechanical [29] properties when compared to the predictable formulation of similar resources. Silver nanoparticles are mostly used. These nanoparticles are used in chemotherapy, medical devices, wound dressing, food additives, water purification, fabrications, textiles, cosmetics, antimicrobial agents, etc. Every day the usage of silver nanoparticles slightly increased for their valuable applicability. Many researchers reported the toxic effect of nanoparticles increased day by day. Silver nanoparticles are widely used particles for various purposes in all fields of science and engineering. Increasing the nano level in environmental conditions create various toxicological problems as well as silver nanoparticles destroy beneficial microorganisms like bacteria, and fungi, including earthworms and the human environment [30].

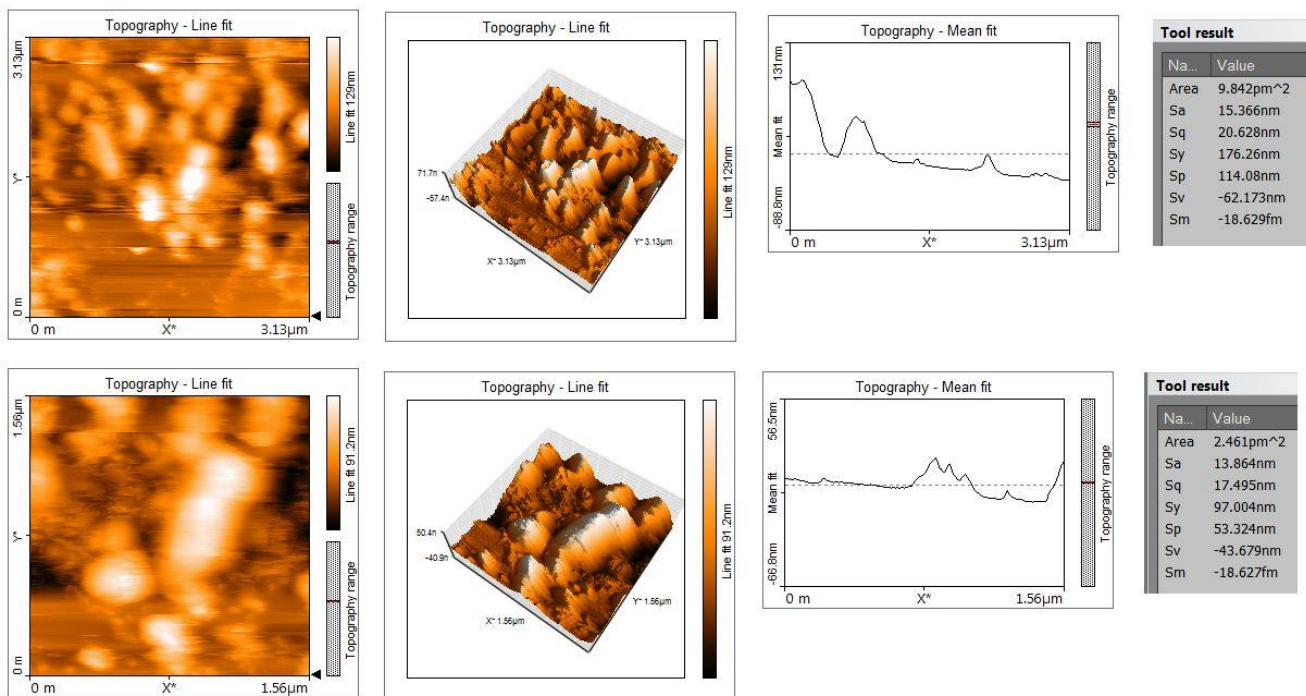


**Fig. 6.** AFM images of green synthesized AgNPs

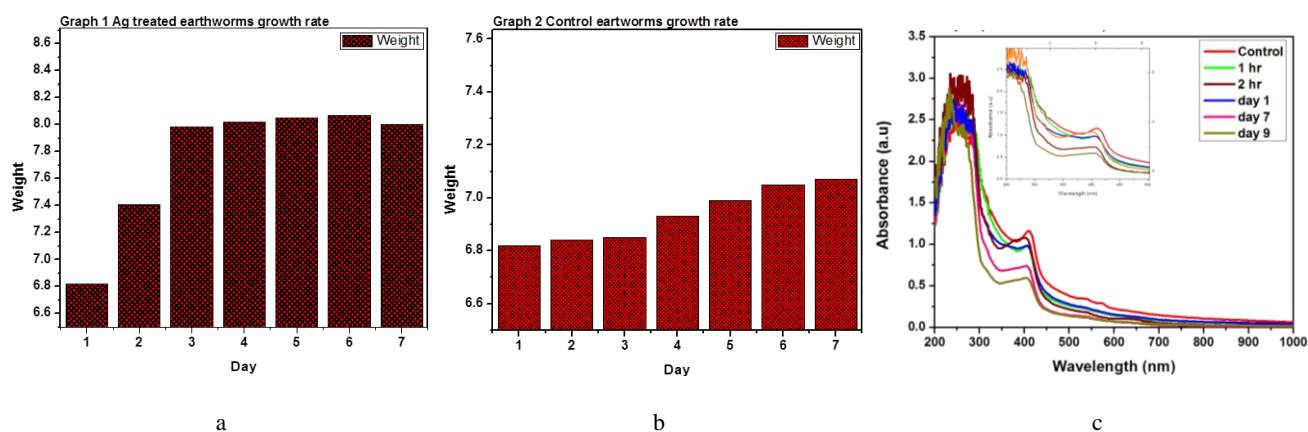


**Fig. 7.** a – silver nanoparticles treated group earthworms growth rate; b – the control group earthworms growth rate; c – UV/Vis spectral data on utilization of plant mediated silver nanoparticles by earthworm body systems

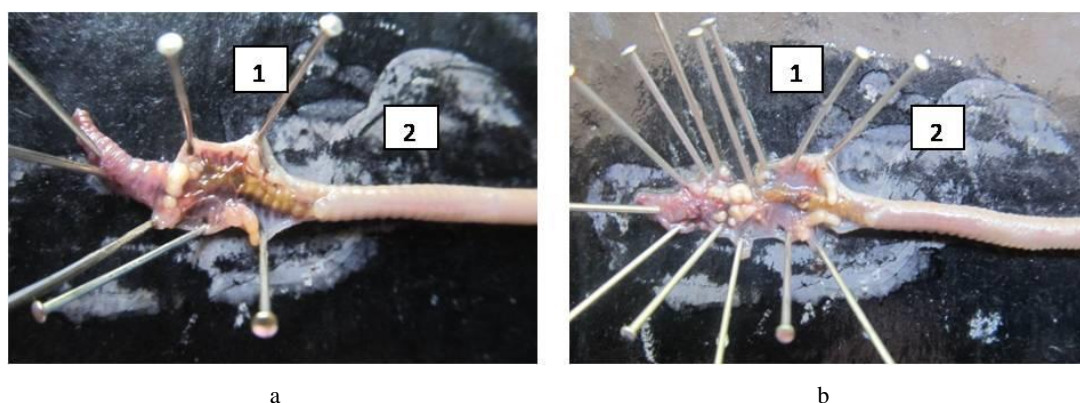


**Fig. 8.** a – dissection of plant mediated silver nanoparticles treated earthworm; b – control earthworm dissection. Label 1: seminal vesicles, Label 2: ovary

#### 4. CONCLUSIONS

In summary, this investigation utilized gas chromatography mass spectrometry (GC-MS) to scrutinize the phytochemical composition of *A. aspera*, revealing a diverse array of over 57 components within the methanol extracts. Dominant constituents such as Neophytadiene, Stigmasterol, 9,19-Cycloergost-24(28)-en-3-ol, 4,14-dimethyl, 22,23-Dibromostigmasterol acetate, 9,19-Cyclolanostan-3-ol, acetate, (3.β.)-Lupeol, and Methyl oleate were identified. The synthesis of silver nanoparticles (AgNPs) via green methods, employing plant extract, was evidenced by a discernible change in color. UV/Vis spectra unveiled absorption peaks at 343 and 411 nm, indicative of surface plasmon resonance (SPR) in the AgNPs. Functional groups on the nanoparticle surface were elucidated through FTIR spectra. X-ray diffraction (XRD) analysis underscored the crystalline nature of the synthesized AgNPs, manifesting as sharp peaks corresponding to crystallographic planes (1 1 1), (2 0 0), (2 2 0), and (3 1 1). The identification of secondary phases, such as  $Ag_3O_4$ , further enriched the understanding of the nanoparticle structure. SEM and AFM images provided a visual representation of the nanoparticles, revealing their spherical shapes and cluster formations. In biological assessments, the introduction of plant-mediated AgNPs into earthworms demonstrated a pronounced enhancement in growth compared to control groups. The investigation into silver content within

earthworms corroborated the observed growth increase, as supported by UV/Vis spectra. Dissection analysis of reproductive organs in earthworms illuminated improved growth in seminal vesicles and ovaries within the treated group. In conclusion, the green-synthesized AgNPs derived from *A. aspera* exhibit distinct properties that positively influence growth and reproductive organs when applied to earthworms. This study highlights the promising applications of plant-mediated nanoparticles in both analytical and biological contexts, showcasing their potential for multifaceted uses.

#### Acknowledgments

This project was supported by Researchers Supporting Project number (RSP2024R315) King Saud University, Riyadh, Saudi Arabia.

#### REFERENCES

1. Bayda, S., Adeel, M., Tuccinardi, T., Cordani, M., Rizzolio, F. The History of Nanoscience and Nanotechnology: From Chemical-Physical Applications to Nanomedicine *Molecules* 25 (1) 2019: pp. 112. <https://doi.org/10.3390/molecules25010112>
2. Sim, S., Wong, N.K. Nanotechnology and its Use in Imaging and Drug Delivery (Review) *Biomedical Reports* 14 (5) 2021: pp. 42. <https://doi.org/10.3892/br.2021.1418>

3. **Yadav, V.K., Malik, P., Khan, A.H., Pandit, P.R., Hasan, M.A., Cabral-Pinto, M.M.S., Islam, S., Suriyaprabha, R., Yadav, K.K., Dinis, P.A., Samreen, H.K., Luisa, D.** Recent Advances on Properties and Utility of Nanomaterials Generated from Industrial and Biological Activities *Crystals* 11 2021: pp. 634. <https://doi.org/10.3390/cryst11060634>
4. **Mariselvam, R., Ignacimuthu, S., Ranjitsingh, A.J.A., Rajapandiyam, K., Mosae Selvakumar, P.** Culture Method-Dependent Variation in the Sensitivity of *Escherichia coli* to Silver Nanoparticles *Advances in Materials Science and Engineering* 2023: pp. 1–6. <https://doi.org/10.1155/2023/1680311>
5. **Mariselvam, R., Ranjitsingh, A.J.A., Usha Raja Nanthini, A., Padmalatha, C., Kalirajan, K., Mosae Selvakumar, P.** Green Synthesis of Silver Nanoparticles from the Extract of the Inflorescence of *Cocos nucifera* (Family: Arecaceae) for Enhanced Antibacterial Activity *Spectrochimica Acta Part A: Molecular and Biomolecular Spectroscopy* 129 2014: pp. 537–541. <https://doi.org/10.1016/j.saa.2014.03.066>
6. **Joudeh, N., Linke, D.** Nanoparticle Classification, Physicochemical Properties, Characterization, and Applications: A Comprehensive Review for Biologists *Journal of Nanobiotechnology* 20 2022: pp. 262. <https://doi.org/10.1186/s12951-022-01477-8>
7. **Altammar, K.A.** A Review on Nanoparticles: Characteristics, Synthesis, Applications, and Challenges *Frontiers in Microbiology* 14 2023: pp. 1155622. <https://doi.org/10.3389/fmicb.2023.1155622>
8. **Xuan, L., Ju, Z., Skonieczna, M., Zhou, P.K., Huang, R.** Nanoparticles-Induced Potential Toxicity on Human Health: Applications, Toxicity Mechanisms, and Evaluation Models *MedComm* 4 (4) 2023: pp. e327. <https://doi.org/10.1002/mco2.327>
9. **Gupta, R., Xie, H.** Nanoparticles in Daily Life: Applications, Toxicity and Regulations *Journal of Environmental Pathology, Toxicology and Oncology : Official Organ of the International Society for Environmental Toxicology and Cancer* 37 (3) 2018: pp. 209–230. <https://doi.org/10.1615/JEnvironPatholToxicolOncol.2018026009>
10. **Manke, A., Wang, L., Rojanasakul, Y.** Mechanisms of Nanoparticle-induced Oxidative Stress and Toxicity *BioMed Research International* 2013: pp. 942916. <https://doi.org/10.1155/2013/942916>
11. **Iravani, S., Korbekandi, H., Mirmohammadi, S.V., Zolfaghari, B.** Synthesis of Silver Nanoparticles: Chemical, Physical and Biological Methods *Research in Pharmaceutical Sciences* 9 (6) 2014: pp. 385–406.
12. **Slepička, P., Slepičková Kasálková, N., Siegel, J., Kolská, Z., Švorčík, V.** Methods of Gold and Silver Nanoparticles Preparation *Materials* 13 (1) 2019: pp. 1. <https://doi.org/10.3390/ma13010001>
13. **Mariselvam, R., Mariappan, A., Sivakavinesan, M., Israel, V.M.V.E., Ignacimuthu, S.** Production of Silver Nanoparticles from *Atalantia Monophylla* (L) Plant Resin and their Enhanced Antibacterial Efficacy *International Nano Letters* 11 2021: pp. 85–91. <https://doi.org/10.1007/s40089-021-00326-0>
14. **Joudeh, N., Linke, D.** Nanoparticle Classification, Physicochemical Properties, Characterization, and Applications: A Comprehensive Review for Biologists *Journal of Nanobiotechnology* 20 2022: pp. 262. <https://doi.org/10.1186/s12951-022-01477-8>
15. **Liu, J.F., Jang, B., Issadore, D., Tsourkas, A.** Use of Magnetic Fields and Nanoparticles to Trigger Drug Release and Improve Tumor Targeting. Wiley Interdisciplinary Reviews *Nanomedicine and Nanobiotechnology* 11 (6) 2019: pp. e1571. <https://doi.org/10.1002/wnan.1571>
16. **Kumar, B.G., Prakash, K.S.** Nanoelectronics and Photonics for Next-Generation Devices. In: Hussain, C.M., Thomas, S. (eds) *Handbook of Polymer and Ceramic Nanotechnology*. Springer, Cham. 2021. [https://doi.org/10.1007/978-3-030-40513-7\\_53](https://doi.org/10.1007/978-3-030-40513-7_53)
17. **Hussein, H.S.** The State of the Art of Nanomaterials and its Applications in Energy Saving *Bulletin of the National Research Centre* 47 2023: pp. 7. <https://doi.org/10.1186/s42269-023-00984-4>
18. **Mariselvam, R., Ranjitsingh, A.J.A., Mosae Selvakumar, P., Abdullah, A.A., Murugan, A.M.** Spectral Studies of UV and Solar Photo catalytic Degradation of AZO Dye and Textile Dye Effluents Using Green Synthesized Silver Nanoparticles *Bioinorganic Chemistry and Applications* 2016: pp. 1–8.
19. **Abbasi, R., Shineh, G., Mobaraki, M., Sarah, D., Lobat, T.** Structural Parameters of Nanoparticles Affecting their Toxicity for Biomedical Applications: A Review *Journal Nanoparticle Research* 25 2023: pp. 43. <https://doi.org/10.1007/s11051-023-05690-w>
20. **Abdal Dayem, A., Hossain, M.K., Lee, S.B., Kim, K., Saha, S.K., Yang, G.M., Choi, H.Y., Cho, S.G.** The Role of Reactive Oxygen Species (ROS) in the Biological Activities of Metallic Nanoparticles *International Journal of Molecular Sciences* 18 (1) 2017: pp. 120. <https://doi.org/10.3390/ijms18010120>
21. **Shukla, R.K., Badiye, A., Vajpayee, K., Kapoor, N.** Genotoxic Potential of Nanoparticles: Structural and Functional Modifications in DNA *Frontiers in Genetics* 12 2021: pp. 728250. <https://doi.org/10.3389/fgene.2021.728250>
22. **Behzadi, S., Serpooshan, V., Tao, W., Hamaly, M.A., Alkawareek, M.Y., Dreaden, E.C., Brown, D., Alkilany, A.M., Farokhzad, O.C., Mahmoudi, M.** Cellular Uptake of Nanoparticles: Journey Inside the Cell *Chemical Society Reviews* 46 (14) 2017: pp. 4218–4244. <https://doi.org/10.1039/c6cs00636a>
23. **Elsabahy, M., Wooley, K.L.** Cytokines as Biomarkers of Nanoparticle Immunotoxicity *Chemical Society Reviews* 42 (12) 2013: pp. 5552–5576. <https://doi.org/10.1039/c3cs60064e>
24. **Sukhanova, A., Bozrova, S., Sokolov, P., Berestovoy, M., Karaulov, A., Nabiev, I.** Dependence of Nanoparticle Toxicity on Their Physical and Chemical Properties *Nanoscale Research Letters* 13 (1) 2018: pp. 44. <https://doi.org/10.1186/s11671-018-2457-x>
25. **Ferrari, M.** Cancer Nanotechnology: Opportunities and Challenges *Nature Reviews Cancer* 5 2005: pp. 161–171. <https://doi.org/10.1038/nrc1566>
26. **Qin, X.Y., Kim, J.G., Lee, J.S.** Synthesis and Magnetic Properties of Nanostructured Ni–Fe Alloys *Nanostructured Materials* 11 1999: pp. 259–270. [https://doi.org/10.1016/s0965-9773\(99\)00040-9](https://doi.org/10.1016/s0965-9773(99)00040-9)
27. **Vasir, J.K., Reddy, M.K., Labhasetwar, V.D.** Nanosystems in Drug Targeting: Opportunities and Challenges *Current Nanoscience* 1 2005: pp. 47–64. <http://dx.doi.org/10.2174/1573413052953110>

28. **Webster, T.J., Siegel, R.W., Bizios, R.** Osteoblast Adhesion on Nanophase Ceramics *Biomaterials* 20 1999: pp. 1221 – 1227.  
[https://doi.org/10.1016/s0142-9612\(99\)00020-4](https://doi.org/10.1016/s0142-9612(99)00020-4)
29. **Webster, T.J., Ergun, C., Doremus, R.H.** Enhanced Functions of Osteoblasts Onnanophase Ceramics *Biomaterials* 21 2000: pp. 1803 – 1810.  
[https://doi.org/10.1016/s0142-9612\(00\)00075-2](https://doi.org/10.1016/s0142-9612(00)00075-2)
30. **Arora, S., Rajwade, J.M., Paknikar, K.M.** Nanotoxicology and in Vitro Studies: The Need of the Hour *Toxicology and Applied Pharmacology* 258 2012: pp. 151 – 165.  
<https://doi.org/10.1016/j.taap.2011.11.010>



© Rajalakshmi et al. 2024 Open Access This article is distributed under the terms of the Creative Commons Attribution 4.0 International License (<http://creativecommons.org/licenses/by/4.0/>), which permits unrestricted use, distribution, and reproduction in any medium, provided you give appropriate credit to the original author(s) and the source, provide a link to the Creative Commons license, and indicate if changes were made.